

# Linear Response pCCD-Based Methods: LR-pCCD and LR-pCCD+S Approaches for the Efficient and Reliable Modeling of Excited State Properties

Somayeh Ahmadkhani,\* Katharina Boguslawski, and Paweł Tecmer\*



Cite This: <https://doi.org/10.1021/acs.jctc.4c01017>



Read Online

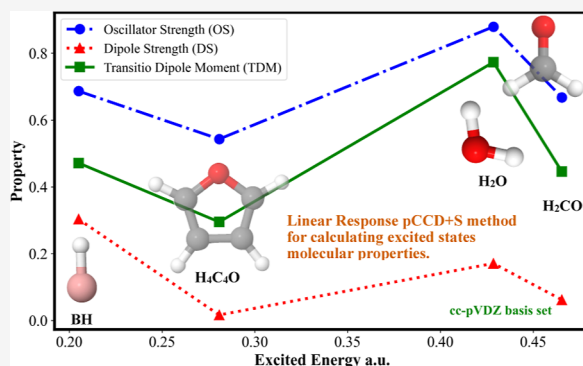
ACCESS |

Metrics & More

Article Recommendations

Supporting Information

**ABSTRACT:** In this work, we derive working equations for the linear response pair coupled cluster doubles (LR-pCCD) ansatz and its extension to singles (S), LR-pCCD+S. These methods allow us to compute electronic excitation energies and transition dipole moments based on a pCCD reference function. We benchmark the LR-pCCD+S model against the linear response coupled-cluster singles and doubles method for modeling electronic spectra (excitation energies and transition dipole moments) of the BH, H<sub>2</sub>O, H<sub>2</sub>CO, and furan molecules. We also analyze the effect of orbital optimization within pCCD on the resulting LR-pCCD+S transition dipole moments and oscillator strengths and perform a statistical error analysis. We show that the LR-pCCD+S method can correctly reproduce the transition dipole moments features, thus representing a reliable and cost-effective alternative to standard, more expensive electronic structure methods for modeling electronic spectra of simple molecules. Specifically, the proposed models require only mean-field-like computational cost, while excited-state properties may approach the CCSD level of accuracy. Moreover, we demonstrate the capability of our model to simulate electronic transitions with non-negligible contributions of double excitations and the electronic spectra of polyenes of various chain lengths, for which standard electronic structure methods perform purely.



Downloaded via NICOLAUS COPERNICUS UNIV TORUN on November 20, 2024 at 12:29:12 UTC.  
See https://pubs.acs.org/sharingguidelines for options on how to legitimately share published articles.

## 1. INTRODUCTION

Electronic spectroscopy plays a pivotal role in various scientific disciplines, from chemistry to physics, biology, and astronomy. Electronic spectra provide a fingerprint of an investigated system. They are crucial for understanding the behavior of electrons in atoms and molecules and the design of new complexes and materials. Experimentally, the electronic spectrum is recorded via absorption or emission processes. The emission spectrum is generated when electrons transition from higher to lower energy levels, emitting photons. The absorption spectrum is produced by electrons absorbing photons to move from lower to higher energy levels. An absorption spectrum is essentially the reverse of an emission spectrum, both provide characteristic molecular features.<sup>1,2</sup>

In recent years, quantum chemistry has become increasingly essential in predicting and interpreting atomic and molecular electronic spectra.<sup>3,4</sup> Two main families of quantum chemistry methods emerged: density functional theory approximations (DFAs) and wave function theory (WFT) based methods. While DFAs are generally more cost-effective, it is well-accepted that WFT provides more reliable results. Specifically, the quality of DFAs' electronic spectra strongly depends on the applied approximation to the exchange–correlation functional. Several classes of approximate exchange–correlation func-

tionals have been developed so far, ranging from the simplest local and semilocal, to hybrid, meta-hybrid, and double-hybrid, to more complex range-separated exchange–correlation functionals.<sup>5</sup> While some of the approximations to the exchange–correlation functional provide reliable results for molecular structures, others perform well in predicting electronic excitation energies.<sup>6,7</sup> However, none of them is universal. Particularly challenging for DFAs are so-called multireference systems with a significant amount of strong electron correlation. Such strongly correlated electrons can be encountered, for instance, when stretching multiple bonds or in extended  $\pi$ -systems.

In WFT, the exact solution to the electronic Schrödinger equation (in a given basis) can be obtained from the full configuration interaction (FCI) approach. Unfortunately, such calculations are computationally feasible only for some small model systems, comprising usually less than 20 electrons and/

Received: August 3, 2024

Revised: October 26, 2024

Accepted: October 30, 2024

or orbitals, as the number of degrees of freedom scales binomially with system size. That technical deficiency led to the development of approximate WFT-based methods (including the hybrid WFT/DFA methods<sup>8</sup>), among which the coupled cluster (CC) theory<sup>9</sup> emerged as the most promising one. Conventional CC theory, like the coupled cluster singles and doubles (CCSD) and CCSD with perturbative triples (CCSD(T)<sup>10</sup>), can be used to accurately model large molecular systems whose electronic structures are well-represented by a single Slater determinant, that is, dominated by dynamic electron correlation effects. The pair coupled-cluster doubles<sup>11,12</sup> (pCCD) model represents a cost-effective alternative for reliable description of strongly correlated systems.<sup>13</sup> Combined with an efficient orbital optimization protocol<sup>14–17</sup> and dynamic energy correction,<sup>18–23</sup> pCCD-based approaches represent a versatile tool for large-scale modeling of complex systems.<sup>24–27</sup>

Employing the equation of motion (EOM) formalism<sup>28–30</sup> on top of a pCCD reference function allows us to obtain a large number of electronically excited states in one single calculation.<sup>31–33</sup> The resulting excitation energies are size-intensive. An advantage of EOM-pCCD-based methods over the standard EOM-CC approaches is the low computational cost and the ability to model electronically excited states of large  $\pi$ -conjugated systems,<sup>34</sup> where the electron pair excitation energies can play a significant role.<sup>31,33</sup> Unfortunately, the computation of oscillator strengths from EOM-CC methods, including the pCCD-based variants, requires the determination of both the right (as for excitation energies) and left eigenvectors of the EOM-CC equations, which essentially doubles the cost of excited-state calculations compared to the calculations of excitation energies only.<sup>29</sup> Alternatively, the electronic spectra can be obtained from the linear response (LR) formulation of CC theory (LR-CC).<sup>35–38</sup> In that case, the excitation energies remain identical with EOM-CC,<sup>38,39</sup> the computation of transition dipole moments still requires left and right eigenvectors, but the resulting transition dipole moments are size-intensive.<sup>38,40</sup> The standard CCSD-based excitation energies can be further corrected for triple excitations using iterative<sup>41</sup> and noniterative techniques.<sup>42,43</sup>

The exceptional performance of EOM-pCCD-based methods for modeling electronic excitation energies of complex systems<sup>31,33,44</sup> and the advantages of the LR-CC formalism motivate us to develop the LR-CC models based on a pCCD reference function (with and without orbital optimization). In this work, we provide working equations for the LR-pCCD and LR-pCCD+S (LR-pCCD with the inclusion of singly excited states) models. Our focus is on excited state properties, not excitation energies, which have been assessed before.<sup>31,33,44</sup> We benchmark the LR-pCCD+S transition dipole moments (TDM) and oscillator strengths (OS) against the LR-CCSD and EOM-CCSD results for small model systems and various basis set sizes. Finally, we show the ability of LR-pCCD+S to model electronic spectra of all *trans*-polyenes of different chain lengths.

## 2. THEORY

**2.1. pCCD Ansatz.** One of the most interesting recent developments in CC theory<sup>9,45,46</sup> is the pCCD ansatz,<sup>11–13</sup> which restricts the coupled cluster wave function ansatz to only electron pair excitations and overall zero-spin

$$|\text{pCCD}\rangle = e^{\hat{T}_{\text{pCCD}}} |\text{HF}\rangle \quad (1)$$

where  $|\text{HF}\rangle$  is some reference determinant (usually the Hartree–Fock determinant) and

$$\hat{T}_{\text{pCCD}} = \sum_{ai} t_{ii}^{a\bar{a}} \hat{P}_a^\dagger \hat{P}_i \quad (2)$$

In the above equation,  $i, j, \dots (a, b, \dots)$  refer to the occupied (virtual) orbitals.  $\hat{P}_q^\dagger = \hat{q}_\uparrow^\dagger \hat{q}_\downarrow^\dagger$  and  $\hat{P}_p = \hat{p}_\downarrow \hat{p}_\uparrow$  are general pair creation ( $\hat{P}_q^\dagger$ ) and annihilation operators ( $\hat{P}_p$ ), respectively. pCCD represents a computationally attractive size-extensive model with mean-field-like scaling.<sup>11</sup> The variational orbital optimization<sup>12,14–17</sup> of the corresponding pCCD orbitals is often carried out to recover size-consistency.<sup>47,48</sup>

The pCCD state aligns with the weak formulation of the time-independent Schrödinger equation

$$e^{-\hat{T}_{\text{pCCD}}} \hat{H}_0 |\text{pCCD}\rangle = E_0 e^{-\hat{T}_{\text{pCCD}}} |\text{pCCD}\rangle \quad (3)$$

that is obtained by projecting the  $\langle \text{HF} |$  state from the left-hand-side as  $E_0 = \langle \text{HF} | \hat{H}_0 | \text{pCCD} \rangle$  and  $\hat{H}_0$  being the molecular Hamiltonian in its normal-product form

$$\hat{H}_0 = \sum_{pq} f_p^q \{ \hat{p}^\dagger \hat{q} \} + \frac{1}{2} \sum_{pqrs} V_{pq}^{rs} \{ \hat{p}^\dagger \hat{q}^\dagger \hat{s} \hat{r} \} \quad (4)$$

where  $f_p^q$  and  $V_{pq}^{rs}$  denote the Fock operator and two-electron integrals, respectively. The pCCD amplitudes,  $t_{ii}^{a\bar{a}}$ , are then obtained by projection

$$\langle \mu | e^{-\hat{T}_{\text{pCCD}}} \hat{H}_0 | \text{pCCD} \rangle = 0 \quad (5)$$

where  $\langle \mu | = \langle \text{HF} | \hat{\tau}_\mu^\dagger$ , and  $\hat{\tau}_\mu^\dagger$  refers to the de-excitation operator, here,  $\hat{P}_i^\dagger \hat{P}_a$ .

**2.2. LR-pCCD and LR-pCCD+S.** The basic response equation for arbitrary operators  $\hat{A}$  and  $\hat{B}$  is given by<sup>36,49</sup>

$$\langle \langle \hat{A}; \hat{B} \rangle \rangle = \sum_k \left\{ \frac{\langle 0 | \hat{A} | k \rangle \langle k | \hat{B} | 0 \rangle}{\omega - \omega_k + i\alpha} - \frac{\langle 0 | \hat{B} | k \rangle \langle k | \hat{A} | 0 \rangle}{\omega + \omega_k + i\alpha} \right\} \quad (6)$$

where  $\langle 0 |$  and  $|k\rangle$  are the ground and excited states, respectively, and  $\alpha$  is a real positive infinitesimal to prevent divergence. Defining  $\langle \Lambda |$  as a dual-type vector to the pCCD wave function

$$\langle \Lambda | = \langle \text{HF} | + \sum_\mu \bar{t}_\mu \langle \bar{\mu}_2 | \quad (7)$$

satisfies the time-independent Schrödinger equation and the normalization condition<sup>36</sup>

$$\langle \Lambda | \hat{H}_0 | \text{pCCD} \rangle = E_0 \quad (8)$$

$$\langle \Lambda | \text{pCCD} \rangle = 1 \quad (9)$$

where the index 2 in  $\langle \mu_2 | = \langle \text{HF} | \hat{\tau}_{\mu_2}^\dagger$  refers to pair de-excitations and  $\bar{t}_\mu$  are the Lagrange multipliers. Considering  $J_{\mu\nu}$  as a Jacobian matrix we will have

$$\sum_\mu \bar{t}_\mu J_{\mu\nu} = \langle \text{HF} | [\hat{H}_0, \hat{\tau}_\nu] | \text{pCCD} \rangle \quad (10)$$

In the presence of an external potential ( $\lambda \hat{V}$ ), applied to a molecular structure with  $\lambda$  intensity, eqs 5, 7, and 10 lead to

**Table 1.** Response Vectors and Matrices for the LR-pCCD and LR-pCCD+S Equations<sup>a</sup>

name	LR-pCCD	LR-pCCD+S
$\bar{A} =$	$e^{-\hat{T}_{pCCD}} \hat{A} e^{\hat{T}_{pCCD}}$	$e^{-\hat{T}_{pCCD}} \hat{A} e^{\hat{T}_{pCCD}}$
$\eta_{\nu}^{\hat{A}} =$	$\langle Hf   [\hat{A}, \hat{\tau}_{\nu_2}]   pCCD \rangle$	$\langle Hf   [\hat{A}, \hat{\tau}_{\nu_1}]   pCCD \rangle$
$\xi_{\mu}^{\hat{A}} =$	$\langle \bar{\mu}_2   \hat{A}   pCCD \rangle$	$\langle \bar{\mu}_1   \hat{A}   pCCD \rangle$
$F_{\mu\nu} =$	$\langle \Lambda   [[\hat{H}_0, \hat{\tau}_{\nu_2}], \hat{\tau}_{\mu_2}]   pCCD \rangle$	$\langle \Lambda   [[\hat{H}_0, \hat{\tau}_{\nu_1}], \hat{\tau}_{\mu_1}]   pCCD \rangle$
		$\langle \Lambda   [[\hat{H}_0, \hat{\tau}_{\nu_2}], \hat{\tau}_{\mu_1}]   pCCD \rangle$
$J_{\mu\nu} =$	$\langle Hf   [[\hat{H}_0, \hat{\tau}_{\nu_2}], \hat{\tau}_{\mu_2}]   pCCD \rangle$	$\langle Hf   [[\hat{H}_0, \hat{\tau}_{\nu_1}], \hat{\tau}_{\mu_2}]   pCCD \rangle$
		$\langle Hf   [[\hat{H}_0, \hat{\tau}_{\nu_2}], \hat{\tau}_{\mu_1}]   pCCD \rangle$

<sup>a</sup>Indices  $n = 1$  and  $n = 2$  refer to single and pair excitations (de-excitation) with respect to the  $\tau_{\mu n}$  ( $\tau_{\nu n}^\dagger$ ) operator. For more details see ref 36.

$$\frac{d}{d\lambda} \langle \Lambda(\lambda) | (\hat{H}_0 + \lambda \hat{V}) | pCCD(\lambda) \rangle |_{\lambda=0} \approx \langle \Lambda | \hat{V} | pCCD \rangle \quad (11)$$

Using the extended Hellmann–Feynman theorem, we can incorporate  $|pCCD\rangle$  and  $\langle \Lambda |$  states into the transition expectation value. According to eq 8, when the cluster operator is not truncated,  $|pCCD\rangle$  and  $\langle \Lambda |$  states represent exact normalized states. However, with a truncated cluster operator,  $\langle \Lambda |$  does not act as the adjoint of  $|pCCD\rangle$ . In this scenario, under the assumption of a time-independent perturbation limit, the response function corresponds to the results of refs 50 and 51 utilizing the Lagrangian technique approach.<sup>36</sup> In our case, the derivatives of molecular orbital coefficients with respect to the perturbation are ignored, and  $\Lambda$  contains the pair excitations only for all models.

The response function for an externally applied time-dependent potential  $\hat{B} \rightarrow \hat{V}_t$  is briefly derived in ref 49 for linear and quadratic terms. Since we are approximating the calculation to the linear part of the response function and using the coupled cluster reference wave function, the derivation of the equations is as follows

$$\begin{aligned} \langle \langle \hat{A}; \hat{V}^\omega \rangle \rangle &= \sum_n Y_n(\omega + i\alpha) \langle \bar{n} | \hat{A} | pCCD \rangle \\ &\quad + \sum_n X_n(\omega + i\alpha) \langle \Lambda | [\hat{A}, \hat{\tau}_n] | pCCD \rangle \end{aligned} \quad (12)$$

where  $\hat{V}^\omega$  is the Fourier transformation of the time-dependent potential  $\hat{V}_t = \int \exp(-i(\omega + i\alpha)t) \hat{V}^\omega d\omega$ . Assuming the diagonalization of the nonsymmetric Jacobian matrix

$$J_{nm} = (U^{-1} \hat{A} U)_{nm} = \delta_{nm} \omega_n \quad (13)$$

the de-excited and excited states can be defined as  $\langle \bar{n} | = \sum_{\nu} U_{n\nu}^{-1} \langle \nu |$  and  $\hat{\tau}_m = \sum_{\mu} \hat{\tau}_{\mu} U_{\mu m}$ , respectively. The  $X$  and  $Y$  vectors in eq 12 are then expressed in terms of the Jacobian matrix and excitation energies ( $\omega$ )

$$X_{\mu}(\omega) = \sum_{\nu} (J + (\omega + i\alpha) I)^{-1}_{\mu\nu} \xi_{\nu} \quad (14)$$

and

$$Y_{\mu}(\omega) = \sum_{\nu} (\langle \Lambda | [\hat{V}^\omega, \hat{\tau}_{\nu}] | pCCD \rangle + \sum_{\gamma} F_{\nu\gamma} X_{\nu}(\omega + i\alpha)) \quad (15)$$

Explicit forms of LR-pCCD and LR-pCCD+S vectors and matrices are collected in Table 1. More details related to the derivation of these vectors and matrices can be found in the Supporting Information.

**2.3. Excitation Energies.** Opposite to the EOM-CC approach, we do not need to diagonalize the effective Hamiltonian to obtain excitation energies using the LR-CC formalism. We should emphasize that the excitation energies and excited states are extracted from the diagonalized Jacobian matrix. It links the eigenvalues of the Jacobian with the underlying excited-state energies and associated eigenvectors with the excited-state wave functions. To clarify this further, we can rewrite the LR function from eq 6 as

$$\langle \langle \hat{A}; \hat{B} \rangle \rangle = \mathbf{A}^{[1]T} (\mathbf{E}^{[2]} - \omega \mathbf{S}^{[2]}) \mathbf{B}^{[1]} \quad (16)$$

where  $\mathbf{A}^{[1]T}$  is the transposed one-dimensional array of  $\hat{A}$  components ( $\langle 0 | \hat{A} | n \rangle, \langle n | \hat{A} | 0 \rangle$ ),  $\mathbf{B}^{[1]} = (\langle n | \hat{B} | 0 \rangle, \langle 0 | \hat{B} | n \rangle)$ , and the term in parentheses provides the excitation energies of the system. By considering this concept, we can rewrite the LR-CC function as follows

$$\langle \langle \hat{A}; \hat{V}^\omega \rangle \rangle = \eta^{\hat{A}} (\mathbf{E}^{[2]} - \omega \mathbf{S}^{[2]}) g^{\hat{V}^\omega} \quad (17)$$

where  $\eta_i^{\hat{A}} = (\langle 0 | [\bar{A}, \hat{\tau}_i] | 0 \rangle, \langle 0 | [\bar{A}, \hat{\tau}_i^\dagger] | 0 \rangle)$ , and  $g_i^{\hat{V}^\omega T} = (\langle 0 | [\bar{V}^\omega, \hat{\tau}_i] | 0 \rangle, \langle 0 | [\bar{V}^\omega, \hat{\tau}_i^\dagger] | 0 \rangle)$ . As a result, we obtain the excitation energies of the system by diagonalizing  $(\mathbf{E}^{[2]} - \omega \mathbf{S}^{[2]})$ , where

$$\mathbf{E}^{[2]} = E_{\mu,\nu} = \begin{pmatrix} \langle 0 | [[\hat{\tau}_{\mu}, \bar{H}_0], \hat{\tau}_{\nu}^\dagger] | 0 \rangle & \langle 0 | [[\hat{\tau}_{\mu}, \bar{H}_0], \hat{\tau}_{\nu}] | 0 \rangle \\ \langle 0 | [[\hat{\tau}_{\mu}^\dagger, \bar{H}_0], \hat{\tau}_{\nu}] | 0 \rangle & \langle 0 | [[\hat{\tau}_{\mu}^\dagger, \bar{H}_0], \hat{\tau}_{\nu}^\dagger] | 0 \rangle \end{pmatrix} \quad (18)$$

and

$$\mathbf{S}^{[2]} = S_{\mu,\nu} = \begin{pmatrix} \langle 0 | [\hat{\tau}_{\mu}, \hat{\tau}_{\nu}^\dagger] | 0 \rangle & \langle 0 | [\hat{\tau}_{\mu}, \hat{\tau}_{\nu}] | 0 \rangle \\ -\langle 0 | [\hat{\tau}_{\mu}^\dagger, \hat{\tau}_{\nu}^\dagger] | 0 \rangle & -\langle 0 | [\hat{\tau}_{\mu}^\dagger, \hat{\tau}_{\nu}] | 0 \rangle \end{pmatrix} \quad (19)$$

The diagonal terms of the  $\mathbf{S}$  matrix contain single excitations and de-excitations. The off-diagonal terms of  $\mathbf{S}$  accommodate only pair excitations and de-excitations and are usually small.

Let us now consider the molecular Hamiltonian in its normal-product form  $\hat{H}_0$  instead of the  $\hat{A}$  operator and represent the  $\hat{B}$  operator by any external potential operator. Now, eq 17 can be simplified such that  $\mathbf{E}$  will refer to the

Jacobian matrix, and S would become the identity matrix (see also eq (4.36) of ref 38). Specifically for the pair and single excitation operators and effective Hamiltonian, the following relations take place

$$\begin{aligned}\hat{\tau}_{\nu_2} &= \hat{P}_b^\dagger \hat{P}_j, \quad \hat{\tau}_{\nu_1} = \hat{b}^\dagger \hat{j} \\ \bar{H}_0 &= e^{-\hat{T}_{\text{pCCD}}} \hat{H}_0 e^{\hat{T}_{\text{pCCD}}} \\ &= \hat{H}_0 + [\hat{H}_0, \hat{T}_{\text{pCCD}}] + \dots\end{aligned}\quad (20)$$

Thus, we can investigate the excitation energies using all standard CC flavors, including pCCD models, by diagonalizing the Jacobian matrix

$$(\mathbf{J} - \omega \mathbf{I}) \mathbf{X} = 0 \quad (21)$$

The explicit Jacobian matrix elements derived for the pCCD and pCCD+S models are provided in the last row of Table 1. To diagonalize such a Jacobian matrix, we can use the nonsymmetric Davidson method.<sup>21,52</sup> We should stress here that EOM-pCCD and LR-pCCD trivially have the same set of eigenvalues (excitation energies) as the diagonalization problems are equivalent. However, EOM-pCCD+S and LR-pCCD+S slightly differ in their excitation spectra as we only consider the Jacobian in the latter, while the former contains a nonzero first column in the effective Hamiltonian to be diagonalized.<sup>31,32</sup> These differences in excitation energies are minor (a few  $\mu E_h$ ) and orders of magnitude smaller than the accuracy of excitation energies.

**2.4. Transition Matrix Elements.** To study the excited state's properties, we need to align the excitation properties with those of the ground state. For that purpose, we use transition matrices that transfer specific ground state operator effects to the excited states. We need the excitation energies and vectors derived in Section 2.3 to achieve that.

The linear response function of eq 6 exhibits poles at energies  $\pm \omega_k$ . By evaluating the residues of these poles, we can straightforwardly obtain transition matrix elements. That involves approximating the frequencies of the linear response function in eq 12 by the pole values, leading to the following relation

$$\begin{aligned}\langle 0|\hat{A}|k\rangle \langle k|\hat{B}|0\rangle &= \lim_{\omega \rightarrow \omega_k} (\omega - \omega_k) \langle \langle \hat{A}; \hat{B} \rangle \rangle \\ &= \lim_{\omega \rightarrow \omega_k} (\omega - \omega_k) \{ \langle \Lambda | [\hat{A}, \hat{\tau}_k] | \text{pCCD} \rangle \\ &\quad - \sum_{nv} \langle \bar{n} | \hat{A} | \text{pCCD} \rangle (\omega - \omega_n)^{-1} F_{vk} \\ &\quad + \langle \Lambda | [\hat{A}, \hat{\tau}_k] | \text{pCCD} \rangle - \sum_k X_\nu^{\hat{A}}(-\omega_k) F_{vk} \} \\ &\langle k|\hat{B}|0\rangle\end{aligned}\quad (22)$$

where  $n$  is the total number of roots,  $k$  denotes the eigenvector, and  $\nu$  is the index of Jacobian matrix element. The above transition matrix could be written as

$$\begin{aligned}\langle 0|\hat{A}|k\rangle \langle k|\hat{B}|0\rangle &= \{ \langle \Lambda | [\hat{A}, \hat{\tau}_k] | \text{pCCD} \rangle - \\ &\quad \sum_\nu (-\mathbf{J} + \omega \mathbf{I})_{\mu\nu}^{-1} \langle \bar{\nu} | \hat{A} | \text{pCCD} \rangle \langle \Lambda | [\hat{H}_0, \hat{\tau}_\nu], \hat{\tau}_k \rangle \\ &\quad | \text{pCCD} \rangle \} \langle k|\hat{B}|0\rangle\end{aligned}\quad (23)$$

where  $\hat{A}$  and  $\hat{B}$  are arbitrary operators,  $\hat{H}_0$  the Hamiltonian of eq 4,  $\mathbf{J}$  is the coupled cluster Jacobian, and  $|\text{pCCD}\rangle$  denotes the pCCD wave function (in the canonical or pCCD orbital basis). The operators  $\hat{A}$  and  $\hat{B}$  can define various properties such as transition dipole moment (TDM), polarizability,<sup>53,54</sup> and excited density matrix (EDM), among others.

**2.5. Transition Dipole Moment and Related Properties.** The TDM, in the absence of any external potential, can be obtained using only the  $\hat{A}$ -dependent part of eq 23 according to the following equation

$$\begin{aligned}\Gamma_{0 \rightarrow k}^{\hat{A}} &= \langle 0 | \hat{A} | k \rangle \\ \langle \Lambda | [\hat{A}, \hat{\tau}_k] | \text{pCCD} \rangle - \sum_\nu &(-\mathbf{J} + \omega \mathbf{I})_{\mu\nu}^{-1} \langle \bar{\nu} | \hat{A} | \text{pCCD} \rangle \\ \langle \Lambda | [[\hat{H}_0, \hat{\tau}_\nu], \hat{\tau}_k] | \text{pCCD} \rangle\end{aligned}\quad (24)$$

Using dipole operators, we can obtain the TDM of selected excited states. An intrinsic feature of choosing pCCD as the reference wave function—in contrast to CCSD-based approaches—is that the Jacobian becomes approximately symmetric, and we can approximate transition dipole moment using only the right eigenvectors without significantly deteriorating the accuracy. This approximation allows us to keep the computational cost to  $O(o^2 v^2)$  (see below). Similarly, the oscillator strength (OS) and dipole strength (DS) can be determined using eq 24 and the following relations

$$\text{OS} = \frac{2}{3} \omega_k \Gamma_{0 \rightarrow k}^{\hat{A}} \Gamma_{0 \rightarrow k}^{\hat{A}} \quad (25)$$

$$\text{DS} = \Gamma_{0 \rightarrow k}^{\hat{A}} \Gamma_{0 \rightarrow k}^{\hat{A}} \quad (26)$$

where  $\omega_k$  are the eigenvalues of the Jacobian (excitation energies), and  $\Gamma_{0 \rightarrow k}^{\hat{A}}$  refers to the TDM elements.

**2.6. Computational Scaling.** Our pCCD-based linear response models feature a formal computational scaling of  $O(o^2 v^2)$  (with some prefactor), neglecting the 4-index transformation of the electron repulsion integrals (ERI), which can be further reduced by working with Cholesky-decomposed ERI. Thus, our LR-pCCD-based models are computationally more efficient than the standard LR-CCSD or EOM-CCSD models, which are of the order of  $O(o^2 v^4)$ . Furthermore, we can store the whole Jacobian (in principle, we can also exactly diagonalize it and have access to all eigenvalues and—left and right—eigenvectors) as it scales as  $O(2o^2 v^2)$  in terms of memory.

### 3. COMPUTATIONAL DETAILS

All pCCD-based calculations were performed in the developer version of the PyBEST v2.1.0.dev0 software package.<sup>24,55</sup> The structural parameters for the small molecules ( $\text{H}_2\text{O}$ ,  $\text{BH}$ ,  $\text{H}_2\text{CO}$ , and furan) were taken from refs 56 and 57. We computed vertical excitation energies for these systems and explored different basis set variants ranging from cc-pVDZ to cc-pVQZ<sup>58</sup> and aug-cc-pVTZ.<sup>59</sup> To compare vertical excitation energies with a double electron transfer character to the CC2 and CC3 literature data, we employed the def2-TZVP basis sets.<sup>60</sup> The  $1\text{A}_g^-$  ( $S_0$ ) ground state structures of all-trans polyenes were taken from ref 61. For these systems, we used a cc-pVDZ basis set.

In all our LR-pCCD+S calculations, we used the frozen core approximation (1s orbitals of C, O, and N were kept frozen)

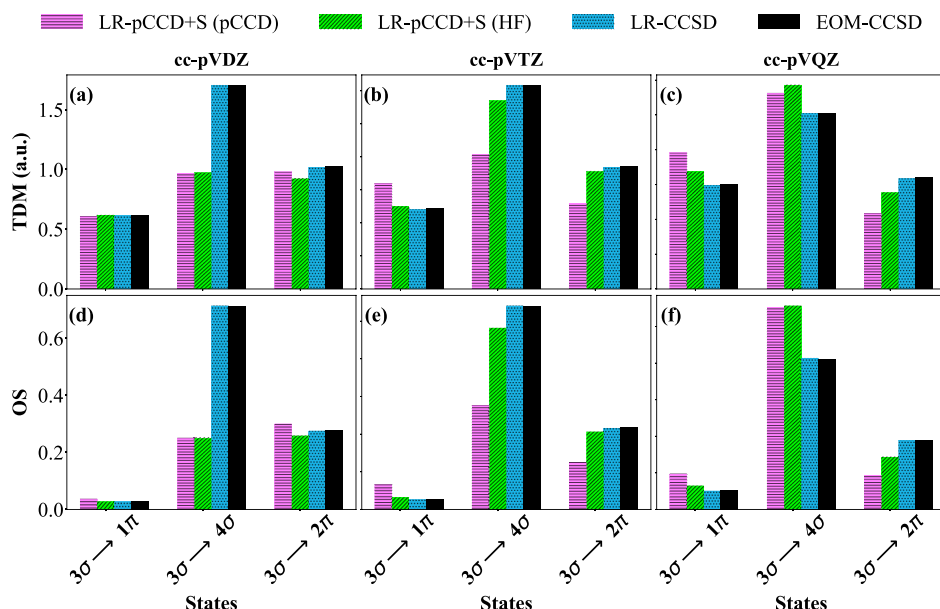


**Figure 1.** LR-pCCD+S(HF), LR-pCCD+S(pCCD), LR-CCSD, and EOM-CCSD TDM and OS for the low-lying excited states of the BH molecule using the cc-pVDZ, cc-pVTZ, and cc-pVQZ basis sets. The LR-pCCD+S(HF) and LR-pCCD+S(pCCD) correspond to LR-pCCD+S calculations using canonical HF and variational orbital-optimized pCCD orbitals, respectively.

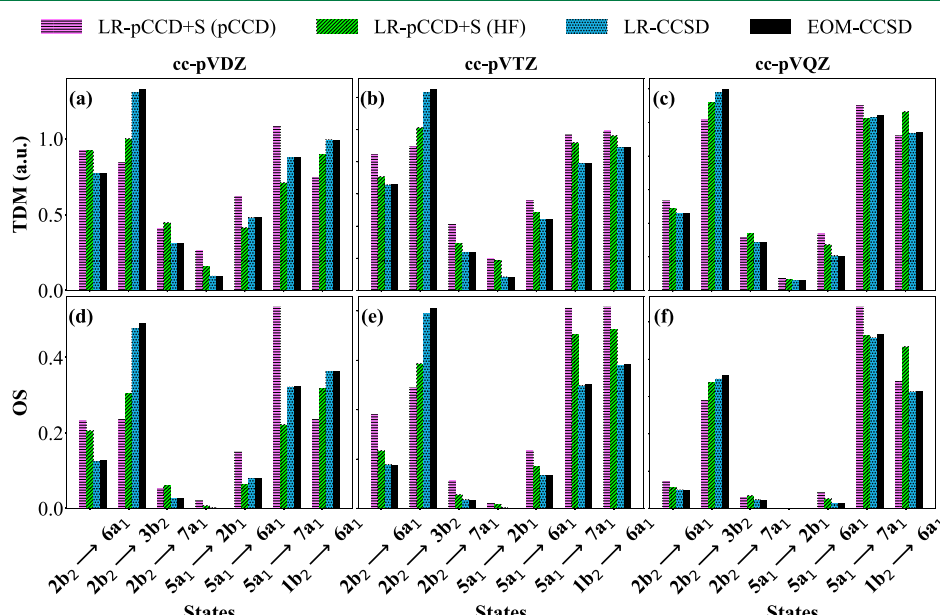


**Figure 2.** LR-pCCD+S(HF), LR-pCCD+S(pCCD), LR-CCSD, and EOM-CCSD TDM and OS for the low-lying excited states of the  $\text{H}_2\text{CO}$  molecule using the cc-pVDZ, cc-pVTZ, and cc-pVQZ basis sets. The LR-pCCD+S(HF) and LR-pCCD+S(pCCD) correspond to LR-pCCD+S calculations using canonical HF and variational orbital-optimized pCCD orbitals, respectively.

and tested two orbital sets: the canonical HF orbitals and the natural pCCD-optimized orbitals. For the latter, we employed a variation orbital optimization protocol<sup>14,17</sup> as implemented in PyBEST.

The reference EOM-CCSD calculations were carried out in the MOLPRO2020 software package<sup>62–64</sup> and the reference LR-CCSD and CCSDR(3) calculations<sup>42</sup> in the DALTON2020 software package<sup>65,66</sup> utilizing the same basis sets and structures as in PyBEST.

#### 4. RESULTS AND DISCUSSION

In this section, we assess the quality of LR-pCCD+S TDMs (eq 24), OSs (eq 25), and DSSs (Supporting Information) (eq

26) by comparing them to other well-established quantum chemistry methods (EOM-CCSD and LR-CCSD) and when possible to experiment. Our analysis is divided into three parts: (a) molecules with a dominant single electron transfer, (b) molecules with a significant admixture of double electron excitations, and (c) polymer chains.

**4.1. Single Electron Excitation Energies.** We start our excited state property analysis by modeling electronic spectra using LR-CCSD and EOM-CCSD as reliable references, for which, triple excitations have negligible effects (see Tables S1–S4 of the Supporting Information). Specifically, we focus on the TDMs and OSs of the low-lying excited states of BH, water ( $\text{H}_2\text{O}$ ), formaldehyde ( $\text{H}_2\text{CO}$ ), and furan ( $\text{C}_4\text{H}_4\text{O}$ ) using

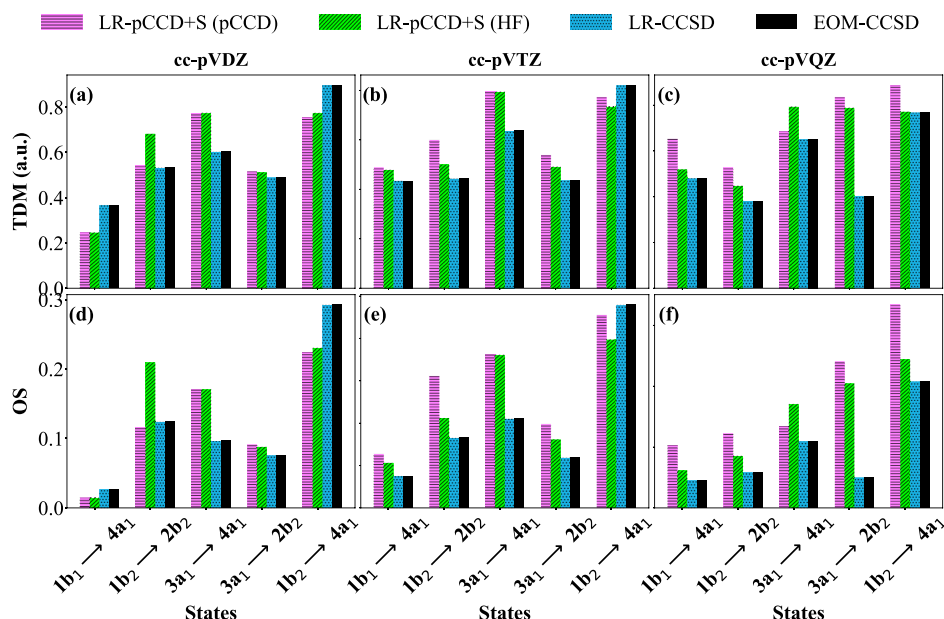


**Figure 3.** LR-pCCD+S(HF), LR-pCCD+S(pCCD), LR-CCSD, and EOM-CCSD TDM and OS for the low-lying excited states of the H<sub>2</sub>O molecule using the cc-pVDZ, cc-pVTZ, and cc-pVQZ basis sets. The LR-pCCD+S(HF) and LR-pCCD+S(pCCD) correspond to LR-pCCD+S calculations using canonical HF and variational orbital-optimized pCCD orbitals, respectively.

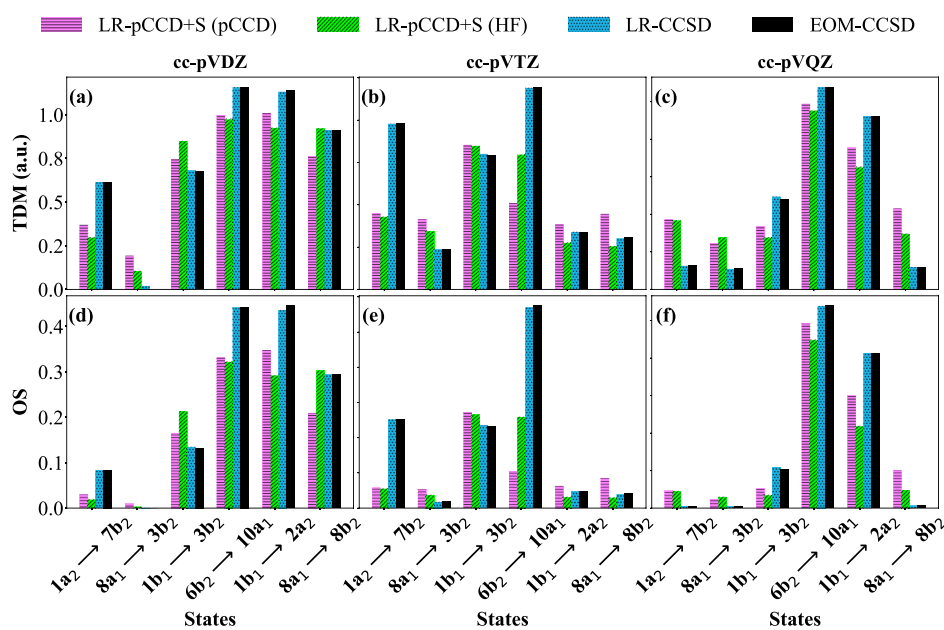


**Figure 4.** LR-pCCD+S(HF), LR-pCCD+S(pCCD), LR-CCSD, and EOM-CCSD TDM and OS for the low-lying excited states of the furan (C<sub>4</sub>H<sub>4</sub>O) molecule using the cc-pVDZ, cc-pVTZ, and cc-pVQZ basis sets. The LR-pCCD+S(HF) and LR-pCCD+S(pCCD) correspond to LR-pCCD+S calculations using canonical HF and variational orbital-optimized pCCD orbitals, respectively.

different basis sets. We investigate two sets of LR-pCCD+S calculations, one where we utilize the HF canonical orbitals and the other where we employ the natural pCCD orbitals (denoted as LR-pCCD+S(HF) and LR-pCCD+S(pCCD), respectively). The performance of LR-pCCD results for these systems is illustrated in Figure 1–4. The corresponding numerical data, including excitation energies, TDMs, OSs, and DSs, are provided in Tables S1–S4 of the Supporting Information.

For the BH molecule, shown in Figure 1, the first ( $3\sigma \rightarrow 1\pi$ ) and third ( $3\sigma \rightarrow 2\pi$ ) electronic transitions exhibit almost the same excited state properties, while the second transition ( $3\sigma$

$\rightarrow 4\sigma$ ) shows the largest values for TDM and OS. However, when the basis set is changed from cc-pVDZ to cc-pVTZ to cc-pVQZ, the difference in second excited state decreases, and LR-pCCD+S approaches LR-CCSD and EOM-CCSD.

Similarly, a good agreement is obtained for the formaldehyde molecule, where the canonical HF LR-pCCD+S excited state properties agree very well with the reference LR-CCSD and EOM-CCSD values and trends for all investigated basis sets (cf. Figure 2). Figure 2 highlights the small deviations occurring between methods even for larger basis set sizes.

We observe a somehow stronger excited-states property dependence on the basis set for the water and furan molecules shown in Figures 3 and 4, respectively. Specifically, the TDMs and OSs quantitatively change when moving from the cc-pVQZ to the cc-pVTZ basis set. Nonetheless, LR-pCCD+S predicts a qualitatively correct picture of TDMs and derived properties (OS) for all excited states. We should stress here that this is not always the case for the augmented basis functions (see Figure S1 of the Supporting Information).

A statistical analysis of the LR-pCCD+S excited state properties is summarized in Table 2. SD and MAE are the

**Table 2. Summary of Statistical Analysis of the LR-pCCD+S Excited State Properties w.r.t the LR-CCSD Reference<sup>a</sup>**

property	SD (pCCD)	SD (HF)	MAE (pCCD)	MAE (HF)
TDM	0.0249	0.0156	0.0459	0.0327
OS	0.0111	0.0083	0.0210	0.0151

<sup>a</sup>SD(HF) and SD(pCCD) denote the standard deviation ( $SD = \sqrt{\frac{\sum_i^N (x_i^{\text{method}} - \bar{x}_i)^2}{N}}$ ) using the canonical HF and the natural pCCD orbitals, respectively, while MAE indicates the mean absolute errors ( $MAE = \frac{1}{N} \sum_i^N |x_i^{\text{method}} - x_i^{\text{ref}}|$ ) using HF and pCCD orbitals. The data corresponds to all molecules, excited states, and basis sets. See also Table S5 of the Supporting Information for statistical analysis for each individual basis set.

smallest for the LR-pCCD+S(HF) approach, indicating that, on average, the canonical HF orbitals provide a slightly better basis than the natural pCCD orbitals for LR-pCCD+S excited state properties (TDMs and OSs). This observation aligns with what has already been observed for pCCD-based electronic excitation energies, suggesting that the ground-state pCCD orbitals might not be optimal for excited-state calculations<sup>31</sup> (as to be expected). Notably, the OS, which depends directly on the excitation energy (cf. eq 25), shows no significant deviations from the statistical errors of TDMs. Table S5 of the Supporting Information dissects the statistical analysis by individual molecules and basis sets, providing a deeper look into their structure and basis set dependence. The largest statistical difference (SD and MAE) between the HF and pCCD bases is observed for the BH molecule.

In summary, by averaging over the basis sets and molecules summarized in Table S5, our in-depth comparison of the LR-pCCD+S approaches to LR-CCSD indicates LR-pCCD+S(HF) as the most reliable method for modeling singly excited state properties of simple molecules (see Table 2 for statistics). Changing the canonical HF basis to the natural, symmetry-broken pCCD-optimized one increases errors (SD and MAE) from about 1 to 2%, while the MAE for the TDM is 3 to 5%.

**4.2. Double Electron Excitations.** In the following, we focus on electronic excitations with a non-negligible double electron transfer character and their OSs. Specifically, we investigate the performance of the LR-pCCD+S methods in modeling the  $2^1A_1$  excited state of furan, cyclopentadiene, and pyridine. These are well-known, challenging examples for excited-state electronic structure methods. The CC2, CASSCF, and CC3 methods are often used to probe the percentage of double electron transfer in these systems.<sup>67</sup> As a reference for our LR-pCCD+S approaches, we use the CC3 method,<sup>68</sup> but we also report the CC2 results for comparison with our approach. We should stress, however, that the pure double-

double excitation block of the CC2 Jacobian is only of zeroth order, meaning it is diagonal and consists solely of orbital energy differences. As a result, excitations dominated by singles are accurate up to the second order in CC2, whereas pure double excitations are accurate only to the zeroth order.<sup>67</sup> Also, similar to EOM-pCCD+S, LR-pCCD+S treats the double electronic transitions approximately, which are limited to the seniority zero sector.<sup>12</sup> Despite their questionable performance for excited states with double excitation character, we will employ CC2 and CC3 as an indication measure for the presented LR-pCCD+S methods.

Our LR-pCCD+S results are summarized in Table 3. Despite overestimating the excitation energies, LR-pCCD+S

**Table 3.  $2^1A_1 (\pi \rightarrow \pi^*)$  Vertical Excitation Energies (EEs) and Oscillator Strengths (OSs) of Furan, Cyclopentadienyl, and Pyridine Using a def2-TZVP Basis Set<sup>a</sup>**

	molecule	LR-pCCD+S(HF)	CC2 <sup>67</sup>	CC3 <sup>68</sup> ( $R_2$ ) <sup>69</sup>
EE	furan	7.95 (4%)	6.75	6.57 (16%)
	cyclopentadiene	7.47 (56%)	7.05	6.28 (22%)
	pyridine	6.44 (8%)	6.88	6.59 (7%)
OS	furan	0.021	0.003	0.001
	cyclopentadiene	0.004	0.011	0.005
	pyridine	0.024	0.021	0.014

<sup>a</sup>The values in parentheses represent the double excitation contributions ( $R_2$  or  $R_p$ ).

predicts oscillator strengths that agree well with the reference CC3 values for cyclopentadiene and pyridine. The only exception is the doubly excited state of the furan molecule. Most likely, this doubly excited state has non-negligible contributions from broken-pair excitations, as the LR-pCCD+S-based percentage contribution of  $R_2$  (more precisely,  $R_p$ ) is very low compared to other methods. Finally, similar to what we have observed earlier, the canonical HF orbital basis provides a more reliable description of LR-pCCD+S excited states and their properties than its pCCD counterpart.

**4.3. All-trans-polyenes.** Finally, we move toward larger molecular structures to further validate our methods and investigate all-trans polyenes,  $C_{2n}H_{2n+2}$ , of different chain lengths with  $n = 5, 6, 7, 8$ . Specifically, we focus on the  $1^1B_u^+$  state, which is known to have a non-negligible intensity and thus to be optically active. We used our LR-pCCD+S(HF) approach to determine the excitation energies and the corresponding OSs and TDMs. As previously reported,<sup>31,32</sup> EOM-pCCD+S(HF) provides reliable excitation energies for the lowest-lying  $1^1B_u^+$  state in these challenging systems. In this work, we turn our attention toward the corresponding excited state properties obtained from the proposed LR-pCCD-based models. To the best of our knowledge, the excited state properties of longer all-trans polyenes have not yet been studied with more elaborate ab initio methods.

Our results for the S0 structures are collected in Table 4. For longer chains, the oscillator strength follows a decreasing trend of excitation energies of the  $1^1B_u^+$  state. The TDMs and OSs reach their minima for the  $C_{14}H_{16}$  molecule. Since there is no other reliable theoretical data to verify our excited state properties, we compare our calculated excitation energies to the experimental spectra from ref 70. Similar to the trends in the oscillator strength predicted with LR-pCCD+S(HF), the experimental intensity decreases toward larger molecules (see Figure 2 of ref 70). Knowing that the LR-pCCD+S(HF)

**Table 4.** LR-pCCD+S Vertical Excitation Energies (EEs), Oscillator Strengths (OSs), and Transition Dipole Moments (TDMs) for the  $1^1\text{B}_u^+$  State in Trans-polyenes

molecule	LR-pCCD+S(HF)			Exp. <sup>70</sup>
	EE (eV)	OS	TDM	EE (eV)
$\text{C}_{10}\text{H}_{12}$	4.91	2.56	0.88	4.60
$\text{C}_{12}\text{H}_{14}$	4.50	1.01	0.58	4.02
$\text{C}_{14}\text{H}_{16}$	4.25	1.00	0.59	3.74
$\text{C}_{16}\text{H}_{18}$	4.00	1.00	0.61	3.51

excited state properties are size intensive and the excitation energies of the  $1^1\text{B}_u^+$  state are reasonable (within the given basis set and molecular structures), we are quite confident that the results in Table 4 are qualitatively correct.

## 5. CONCLUSIONS AND OUTLOOK

In this work, we derived the working equations for the LR-pCCD and LR-pCCD+S methods. While the first one has little use in quantum chemistry applications as it is restricted to pair excited states only, the latter provides a computationally inexpensive extension to the EOM-pCCD+S method,<sup>31,32</sup> allowing us to target excited state properties such as TDMs, OSs, and DSs (see Supporting Information) within the pCCD model, requiring only mean-field-like computational cost. Most importantly, our numerical examples validate the approximate inclusion of single excitations and the restriction to the right eigenstates only. Specifically, our study indicates a satisfyingly good performance of the LR-pCCD+S model for singly excited states, comparable to the LR-CCSD approach and the more expensive EOM-CCSD approach (mean-field-like vs  $N^6$  scaling). Similar to EOM-pCCD+S excitation energies, excited state properties within the LR-pCCD+S framework are, on average, more reliable using canonical HF orbitals than the natural pCCD-optimized orbitals. Moreover, we demonstrate that our LR-pCCD+S(HF) method can also be used to predict excited state properties of more complex systems with a significant amount of double/biexcitation character. Our LR-pCCD+S predictions are, however, limited to doubly excited states of seniority zero character. Finally, we provide a first theoretical description of electronic TDMs and OSs for the  $1^1\text{B}_u^+$  state of longer all-trans polyene chains. Specifically, LR-pCCD+S(HF) predicts electronic properties in good agreement with experimentally recorded spectra.

In summary, we introduced a new cost-effective computational protocol representing a robust model to predict excited state properties qualitatively. To reduce the errors with respect to more elaborate models and hence to reach a more quantitative level for the prediction of excited state properties, we must account for the missing dynamic correlation energy in our LR-pCCD+S approach. Promising alternatives are various tailored coupled cluster corrections on top of the pCCD reference function<sup>12,19,23</sup> within the linear response framework. Finally, the pCCD-based transition density matrices open new ways to construct excited states' descriptors and topological analyses of charge transfer excited states<sup>71</sup> that are of great importance in organic electronics.<sup>25,72</sup>

## ■ ASSOCIATED CONTENT

### Data Availability Statement

The data underlying this study are available in the published article and its Supporting Information. The released version of the PyBEST code is available on Zenodo at <https://zenodo.org/record/10069179>.

and on PyPI at <https://pypi.org/project/pybest/>.

### ■ Supporting Information

The Supporting Information is available free of charge at <https://pubs.acs.org/doi/10.1021/acs.jctc.4c01017>.

Tables of data for TDM and OS, and DS results from Molpro and LR-pCCD+S in HF and pCCD base calculations for BH,  $\text{H}_2\text{O}$ ,  $\text{H}_2\text{CO}$ , and furan molecules across different basis sets. Tables of statistical calculations for SD and MAE for individual molecules in various basis sets. A detailed explanation of the calculations used to obtain the final relation for transition matrix elements, including the vectors and matrices referenced in Table 1 (PDF)

## ■ AUTHOR INFORMATION

### Corresponding Authors

Somayeh Ahmadkhani – Institute of Physics, Faculty of Physics, Astronomy, and Informatics, Nicolaus Copernicus University in Toruń, Toruń 87-100, Poland;  [0000-0001-6312-632X](https://orcid.org/0000-0001-6312-632X); Email: [so.ahmadkhani@gmail.com](mailto:so.ahmadkhani@gmail.com)

Paweł Tecmer – Institute of Physics, Faculty of Physics, Astronomy, and Informatics, Nicolaus Copernicus University in Toruń, Toruń 87-100, Poland;  [0000-0001-6347-878X](https://orcid.org/0000-0001-6347-878X); Email: [ptecmer@fizyka.umk.pl](mailto:ptecmer@fizyka.umk.pl)

### Author

Katarzyna Boguslawski – Institute of Physics, Faculty of Physics, Astronomy, and Informatics, Nicolaus Copernicus University in Toruń, Toruń 87-100, Poland;  [0000-0001-7793-1151](https://orcid.org/0000-0001-7793-1151)

Complete contact information is available at: <https://pubs.acs.org/10.1021/acs.jctc.4c01017>

### Notes

The authors declare no competing financial interest.

## ■ ACKNOWLEDGMENTS

S.A. and P.T. acknowledge financial support from the SONATA BIS research grant from the National Science Centre, Poland (grant no. 2021/42/E/ST4/00302). Funded/Co-funded by the European Union (ERC, DRESSED-pCCD, 101077420). Views and opinions expressed are, however, those of the author(s) only and do not necessarily reflect those of the European Union or the European Research Council. Neither the European Union nor the granting authority can be held responsible for them. S.A. gratefully acknowledges Prof. Iulia Emilia Brumboiu for the very helpful discussions.

## ■ REFERENCES

- Baker, A. D.; Brundle, C. R.; Thompson, M. Electron spectroscopy. *Chem. Soc. Rev.* **1972**, *1*, 355–380.
- Harris, D. C.; Bertolucci, M. D. *Symmetry and Spectroscopy. An Introduction to Vibrational and Electronic Spectroscopy*; Dover, 1989.
- Bartlett, R. J. Coupled-cluster approach to molecular structure and spectra: a step toward predictive quantum chemistry. *J. Chem. Phys.* **1989**, *93*, 1697–1708.
- Dreuw, A.; Head-Gordon, M. Single-Reference ab Initio Methods for the Calculation of Excited States of Large Molecules. *Chem. Rev.* **2005**, *105*, 4009–4037.
- Becke, A. D. Perspective: Fifty years of density-functional theory in chemical physics. *J. Chem. Phys.* **2014**, *140*, 18A301.

- (6) Barbatti, M.; Aquino, A. J.; Lischka, H. The UV absorption of nucleobases: semi-classical ab initio spectra simulations. *Phys. Chem. Chem. Phys.* **2010**, *12*, 4959–4967.
- (7) Tecmer, P.; Govind, N.; Kowalski, K.; de Jong, W. A.; Visscher, L. Reliable Modeling of the Electronic Spectra of Realistic Uranium Complexes. *J. Chem. Phys.* **2013**, *139*, 034301.
- (8) Fromager, E.; Knecht, S.; Jensen, H. J. A. Multi-configuration time-dependent density-functional theory based on range separation. *J. Chem. Phys.* **2013**, *138*, 084101.
- (9) Bartlett, R. J.; Musial, M. Coupled-cluster theory in quantum chemistry. *Rev. Mod. Phys.* **2007**, *79*, 291–352.
- (10) Raghavachari, K.; Trucks, G. W.; Pople, J. A.; Head-Gordon, M. A fifth-order perturbation comparison of electron correlation theories. *Chem. Phys. Lett.* **1989**, *157*, 479–483.
- (11) Limacher, P. A.; Ayers, P. W.; Johnson, P. A.; De Baerdemacker, S.; Van Neck, D.; Bultinck, P. A new mean-field method suitable for strongly correlated electrons: computationally facile antisymmetric products of nonorthogonal geminals. *J. Chem. Theory Comput.* **2013**, *9*, 1394–1401.
- (12) Stein, T.; Henderson, T. M.; Scuseria, G. E. Seniority zero pair coupled cluster doubles theory. *J. Chem. Phys.* **2014**, *140*, 214113.
- (13) Tecmer, P.; Boguslawski, K. Geminal-based electronic structure methods in quantum chemistry. Toward a geminal model chemistry. *Phys. Chem. Chem. Phys.* **2022**, *24*, 23026–23048.
- (14) Boguslawski, K.; Tecmer, P.; Ayers, P. W.; Bultinck, P.; De Baerdemacker, S.; Van Neck, D. Efficient description of strongly correlated electrons with mean-field cost. *Phys. Rev. B: Condens. Matter Mater. Phys.* **2014**, *89*, No. 201106(R).
- (15) Limacher, P. A.; Kim, T. D.; Ayers, P. W.; Johnson, P. A.; De Baerdemacker, S.; Van Neck, D.; Bultinck, P. The influence of orbital rotation on the energy of closed-shell wavefunctions. *Mol. Phys.* **2014**, *112*, 853–862.
- (16) Boguslawski, K.; Tecmer, P.; Limacher, P. A.; Johnson, P. A.; Ayers, P. W.; Bultinck, P.; De Baerdemacker, S.; Van Neck, D. Projected seniority-two orbital optimization of the antisymmetric product of one-reference orbital geminal. *J. Chem. Phys.* **2014**, *140*, 214114.
- (17) Boguslawski, K.; Tecmer, P.; Bultinck, P.; De Baerdemacker, S.; Van Neck, D.; Ayers, P. W. Non-variational orbital optimization techniques for the AP1roG wave function. *J. Chem. Theory Comput.* **2014**, *10*, 4873–4882.
- (18) Limacher, P.; Ayers, P.; Johnson, P.; De Baerdemacker, S.; Van Neck, D.; Bultinck, P. Simple and Inexpensive Perturbative Correction Schemes for Antisymmetric Products of Nonorthogonal Geminals. *Phys. Chem. Chem. Phys.* **2014**, *16*, 5061–5065.
- (19) Boguslawski, K.; Ayers, P. W. Linearized Coupled Cluster Correction on the Antisymmetric Product of 1-Reference Orbital Geminals. *J. Chem. Theory Comput.* **2015**, *11*, 5252–5261.
- (20) Boguslawski, K.; Tecmer, P. Benchmark of dynamic electron correlation models for seniority-zero wavefunctions and their application to thermochemistry. *J. Chem. Theory Comput.* **2017**, *13*, 5966–5983.
- (21) Nowak, A.; Boguslawski, K. A configuration interaction correction on top of pair coupled cluster doubles. *Phys. Chem. Chem. Phys.* **2023**, *25*, 7289–7301.
- (22) Garza, A. J.; Bulik, I. W.; Henderson, T. M.; Scuseria, G. E. Range separated hybrids of pair coupled cluster doubles and density functionals. *Phys. Chem. Chem. Phys.* **2015**, *17*, 22412–22422.
- (23) Leszczyk, A.; Máté, M.; Legeza, O.; Boguslawski, K. Assessing the accuracy of tailored coupled cluster methods corrected by electronic wave functions of polynomial cost. *J. Chem. Theory Comput.* **2022**, *18*, 96–117.
- (24) Boguslawski, K.; Leszczyk, A.; Nowak, A.; Brzęk, F.; Żuchowski, P. S.; Kedziera, D.; Tecmer, P. Pythonic Black-box Electronic Structure Tool (PyBEST). An open-source Python platform for electronic structure calculations at the interface between chemistry and physics. *Comput. Phys. Commun.* **2021**, *264*, 107933.
- (25) Tecmer, P.; Galyńska, M.; Szczuczko, L.; Boguslawski, K. Geminal-based strategies for modeling large building blocks of organic electronic materials. *J. Phys. Chem. Lett.* **2023**, *14*, 9909–9917.
- (26) Galyńska, M.; de Moraes, M. M. F.; Tecmer, P.; Boguslawski, K. Delving into the Catalytic Mechanism of Molybdenum Cofactors: A Novel Coupled Cluster Study. *Phys. Chem. Chem. Phys.* **2024**, *26*, 18918–18929.
- (27) Kriebel, M. H.; Tecmer, P.; Galyńska, M.; Leszczyk, A.; Boguslawski, K. Accelerating Pythonic coupled cluster implementations: a comparison between CPUs and GPUs. *J. Chem. Theory Comput.* **2024**, *24*, 1130–1142.
- (28) Rowe, D. J. Equations-of-Motion Method and the Extended Shell Model. *Rev. Mod. Phys.* **1968**, *40*, 153–166.
- (29) Stanton, J. F.; Bartlett, R. J. The equation of motion coupled-cluster method. A systematic biorthogonal approach to molecular excitation energies, transition probabilities, and excited state properties. *J. Chem. Phys.* **1993**, *98*, 7029–7039.
- (30) Bartlett, R. J. Coupled-cluster theory and its equation-of-motion extensions. *Wiley Interdiscip. Rev.: Comput. Mol. Sci.* **2012**, *2*, 126–138.
- (31) Boguslawski, K. Targeting excited states in all-trans polyenes with electron-pair states. *J. Chem. Phys.* **2016**, *145*, 234105.
- (32) Boguslawski, K. Erratum: “Targeting excited states in all-trans polyenes with electron-pair states” [J. Chem. Phys. 145, 234105 (2016)]. *J. Chem. Phys.* **2017**, *147*, 139901.
- (33) Boguslawski, K. Targeting Doubly Excited States with Equation of Motion Coupled Cluster Theory Restricted to Double Excitations. *J. Chem. Theory Comput.* **2019**, *15*, 18–24.
- (34) Jahani, S.; Boguslawski, K.; Tecmer, P. The relationship between structure and excited-state properties in polyanilines from geminal-based methods. *RSC Adv.* **2023**, *13*, 27898–27911.
- (35) Sekino, H.; Bartlett, R. J. A linear response, coupled-cluster theory for excitation energy. *Int. J. Quantum Chem.* **1984**, *26*, 255–265.
- (36) Koch, H.; Jørgensen, P. Coupled cluster response functions. *J. Chem. Phys.* **1990**, *93*, 3333–3344.
- (37) Koch, H.; Jensen, H. J. A.; Jørgensen, P.; Helgaker, T. Excitation energies from the coupled cluster singles and doubles linear response function (CCSDLR). Applications to Be, CH<sup>+</sup>, CO, and H<sub>2</sub>O. *J. Chem. Phys.* **1990**, *93*, 3345–3350.
- (38) Christiansen, O.; Jørgensen, P.; Hättig, C. Response functions from Fourier component variational perturbation theory applied to a time-averaged quasienergy. *Int. J. Quantum Chem.* **1998**, *68*, 1–52.
- (39) Watts, J. D. *Radiation Induced Molecular Phenomena in Nucleic Acids*; Springer, 2008; pp 65–92.
- (40) Koch, H.; Kobayashi, R.; Sanchez de Merás, A.; Jørgensen, P. Calculation of size-intensive transition moments from the coupled cluster singles and doubles linear response function. *J. Chem. Phys.* **1994**, *100*, 4393–4400.
- (41) Hald, K.; Hättig, C.; Olsen, J.; Jørgensen, P. CC3 triplet excitation energies using an explicit spin coupled excitation space. *J. Chem. Phys.* **2001**, *115*, 3545–3552.
- (42) Christiansen, O.; Koch, H.; Jørgensen, P. Perturbative triple excitation corrections to coupled cluster singles and doubles excitation energies. *J. Chem. Phys.* **1996**, *105*, 1451–1459.
- (43) Christiansen, O.; Koch, H.; Jørgensen, P.; Olsen, J. Excitation energies of H<sub>2</sub>O, N<sub>2</sub> and C<sub>2</sub> in full configuration interaction and coupled cluster theory. *Chem. Phys. Lett.* **1996**, *256*, 185–194.
- (44) Nowak, A.; Tecmer, P.; Boguslawski, K. Assessing the accuracy of simplified coupled cluster methods for electronic excited states in f0 actinide compounds. *Phys. Chem. Chem. Phys.* **2019**, *21*, 19039–19053.
- (45) Čížek, J. On the Correlation Problem in Atomic and Molecular Systems. Calculation of Wavefunction Components in Ursell-Type Expansion Using Quantum-Field Theoretical Methods. *J. Chem. Phys.* **1966**, *45*, 4256–4266.
- (46) Čížek, J.; Paldus, J. Correlation problems in atomic and molecular systems III. Rederivation of the coupled-pair many-electron

- theory using the traditional quantum chemical methods. *Int. J. Quantum Chem.* **1971**, *5*, 359–379.
- (47) Tecmer, P.; Severo Pereira Gomes, A.; Knecht, S.; Visscher, L. Communication: Relativistic Fock-Space Coupled Cluster Study of Small Building Blocks of Larger Uranium Complexes. *J. Chem. Phys.* **2014**, *141*, 041107.
- (48) Brzak, F.; Boguslawski, K.; Tecmer, P.; Żuchowski, P. S. Benchmarking the accuracy of seniority-zero wave function methods for noncovalent interactions. *J. Chem. Theory Comput.* **2019**, *15*, 4021–4035.
- (49) Olsen, J.; Jørgensen, P. Linear and nonlinear response functions for an exact state and for an MCSCF state. *J. Chem. Phys.* **1985**, *82*, 3235–3264.
- (50) Koch, H.; Jensen, H. J.; Helgaker, T.; Scuseria, G. E.; Schaefer, H. F. Coupled cluster energy derivatives. Analytic Hessian for the closed-shell coupled cluster singles and doubles wave function: Theory and applications. *J. Chem. Phys.* **1990**, *92*, 4924–4940.
- (51) Jo/røgensen, P.; Helgaker, T. Møller–Plesset energy derivatives. *J. Chem. Phys.* **1988**, *89*, 1560–1570.
- (52) Cave, R. J.; Davidson, E. R. A theoretical investigation of some low-lying singlet states of 1, 3-butadiene. *J. Chem. Phys.* **1987**, *91*, 4481–4490.
- (53) Pedersen, T. B.; Sánchez de Merás, A. M.; Koch, H. Polarizability and optical rotation calculated from the approximate coupled cluster singles and doubles CC2 linear response theory using Cholesky decompositions. *J. Chem. Phys.* **2004**, *120*, 8887–8897.
- (54) Tucholska, A. M.; Modrzejewski, M.; Moszynski, R. Transition properties from the Hermitian formulation of the coupled cluster polarization propagator. *J. Chem. Phys.* **2014**, *141*, 124109.
- (55) Boguslawski, K.; Brzak, F.; Chakraborty, R.; Cieślak, K.; Jahani, S.; Leszczyk, A.; Nowak, A.; Sujkowski, E.; Świerczyński, J.; Ahmadkhani, S.; Kdziera, D.; Kriebel, M. H.; Żuchowski, P. S.; Tecmer, P. PyBEST: improved functionality and enhanced performance. *Comput. Phys. Commun.* **2024**, *297*, 109049.
- (56) Chrayteh, A.; Blondel, A.; Loos, P.-F.; Jacquemin, D. Mountaineering strategy to excited states: highly accurate oscillator strengths and dipole moments of small molecules. *J. Chem. Theory Comput.* **2021**, *17*, 416–438.
- (57) Loos, P.-F.; Lipparini, F.; Boggio-Pasqua, M.; Scemama, A.; Jacquemin, D. A mountaineering strategy to excited states: Highly accurate energies and benchmarks for medium sized molecules. *J. Chem. Theory Comput.* **2020**, *16*, 1711–1741.
- (58) Dunning, T. H., Jr Gaussian basis sets for use in correlated molecular calculations. I. The atoms boron through neon and hydrogen. *J. Chem. Phys.* **1989**, *90*, 1007–1023.
- (59) Kendall, R. A.; Dunning, T. H.; Harrison, R. J. Electron affinities of the first-row atoms revisited. Systematic basis sets and wave functions. *J. Chem. Phys.* **1992**, *96*, 6796–6806.
- (60) Weigend, F.; Ahlrichs, R. Balanced basis sets of split valence, triple zeta valence and quadruple zeta valence quality for H to Rn: Design and assessment of accuracy. *Phys. Chem. Chem. Phys.* **2005**, *7*, 3297–3305.
- (61) Hu, W.; Chan, G. K.-L. Excited-State Geometry Optimization with the Density Matrix Renormalization Group, as Applied to Polyenes. *J. Chem. Theory Comput.* **2015**, *11*, 3000–3009.
- (62) Werner, H.-J.; Knowles, P. J.; Celani, P.; Györffy, W.; Hesselmann, A.; Kats, D.; Knizia, G.; Köhn, A.; Korona, T.; Kreplin, D.; Lindh, R.; Ma, Q.; Manby, F. R.; Mitrushchenkov, A.; Rauhut, G.; Schütz, M.; Shamasundar, K. R.; Adler, T. B.; Amos, R. D.; Bennie, S. J.; Bernhardsson, A.; Berning, A.; Black, J. A.; Bygrave, P. J.; Cimiraglia, R.; Cooper, D. L.; Coughtrie, D.; Deegan, M. J. O.; Dobbyn, A. J.; Doll, K.; Dornbach, M.; Eckert, F.; Erfort, S.; Goll, E.; Hampel, C.; Hetzer, G.; Hill, J. G.; Hodges, M.; Hrenar, T.; Jansen, G.; Köppel, C.; Kollmar, C.; Lee, S. J. R.; Liu, Y.; Lloyd, A. W.; Mata, R. A.; May, A. J.; Mussard, B.; McNicholas, S. J.; Meyer, W.; Miller, I. I. T. F.; Mura, M. E.; Nicklass, A.; O’Neill, D. P.; Palmieri, P.; Peng, D.; Peterson, K. A.; Pflüger, K.; Pitzer, R.; Polyak, I.; Reiher, M.; Richardson, J. O.; Robinson, J. B.; Schröder, B.; Schwick, M.; Shiozaki, T.; Sibaev, M.; Stoll, H.; Stone, A. J.; Tarroni, R.; Thorsteinsson, T.;
- Toulouse, J.; Wang, M.; Welborn, M.; Ziegler, B. MOLPRO, version 2020.2.1, a package of *ab initio* programs. 2020, <http://www.molpro.net> (accessed March 1, 2024).
- (63) Werner, H.-J. W.; Knowles, P. J.; Manby, F. R.; Black, J. A.; Doll, K.; Hefelmann, A.; Kats, D.; Köhn, A.; Korona, T.; Kreplin, D. A.; Ma, Q.; Miller, T. F., III; Mitrushchenkov, A.; Peterson, K. A.; Polyak, I.; Rauhut, G.; Sibaev, M. The Molpro quantum chemistry package. *J. Chem. Phys.* **2020**, *152*, 144107.
- (64) Werner, H.-J.; Knowles, P. J.; Knizia, G.; Manby, F. R.; Schütz, M. Molpro: A General Purpose Quantum Chemistry Program Package. *Wiley Interdiscip. Rev.: Comput. Mol. Sci.* **2012**, *2*, 242–253.
- (65) Aidas, K.; Angeli, C.; Bak, K. L.; Bakken, V.; Bast, R.; Boman, L.; Christiansen, O.; Cimiraglia, R.; Coriani, S.; Dahle, P.; Dalskov, E. K.; Ekström, U.; Enevoldsen, T.; Eriksen, J. J.; Ettenhuber, P.; Fernández, B.; Ferrighi, L.; Fliegl, H.; Frediani, L.; Hald, K.; Halkier, A.; Hättig, C.; Heiberg, H.; Helgaker, T.; Hennum, A. C.; Hettema, H.; Hjertenæs, E.; Host, S.; Høyvik, I.-M.; Iozzi, M. F.; Jansik, B.; Jensen, H. J. A.; Jonsson, D.; Jørgensen, P.; Kauczor, J.; Kirpekar, S.; Kjærgaard, T.; Klopper, W.; Knecht, S.; Kobayashi, R.; Koch, H.; Kongsted, J.; Krapp, A.; Kristensen, K.; Ligabue, A.; Lutnæs, O. B.; Melo, J. I.; Mikkelsen, K. V.; Myhre, R. H.; Neiss, C.; Nielsen, C. B.; Norman, P.; Olsen, J.; Olsen, J. M. H.; Østed, A.; Packer, M. J.; Pawłowski, F.; Pedersen, T. B.; Provasi, P. F.; Reine, S.; Rinkevicius, Z.; Ruden, T. A.; Ruud, K.; Rybkin, V. V.; Salek, P.; Samson, C. C. M.; de Merás, A. S.; Saue, T.; Sauer, S. P. A.; Schimmelpfennig, B.; Sneskov, K.; Steindal, A. H.; Sylvester-Hvid, K. O.; Taylor, P. R.; Teale, A. M.; Tellgren, E. I.; Tew, D. P.; Thorvaldsen, A. J.; Thøgersen, L.; Vahtras, O.; Watson, M. A.; Wilson, D. J. D.; Ziolkowski, M.; Ågren, H. The Dalton Quantum Chemistry Program System. *Wiley Interdiscip. Rev.: Comput. Mol. Sci.* **2014**, *4*, 269–284.
- (66) Dalton, a molecular electronic structure program, Release v2020.0. 2020, <http://daltonprogram.org>.
- (67) Schreiber, M.; Silva-Junior, M. R.; Sauer, S. P. A.; Thiel, W. Benchmarks for electronically excited states: CASPT2, CC2, CCSD, and CC3. *J. Chem. Phys.* **2008**, *128*, 134110.
- (68) Sauer, S. P. A.; Pitzner-Frydendahl, H. F.; Buse, M.; Jensen, H. J. A.; Thiel, W. Performance of SOPPA-based methods in the calculation of vertical excitation energies and oscillator strengths. *Mol. Phys.* **2015**, *113*, 2026–2045.
- (69) Sauer, S. P. A.; Schreiber, M.; Silva-Junior, M. R.; Thiel, W. Benchmarks for electronically excited states: a comparison of noniterative and iterative triples corrections in linear response coupled cluster methods: CCSDR(3) versus CC3. *J. Chem. Theory Comput.* **2009**, *5*, 555–564.
- (70) Christensen, R. L.; Galinato, M. G. I.; Chu, E. F.; Howard, J. N.; Broene, R. D.; Frank, H. A. Energies of low-lying excited states of linear polyenes. *J. Phys. Chem. A* **2008**, *112*, 12629–12636.
- (71) Etienne, T. Transition matrices and orbitals from reduced density matrix theory. *J. Chem. Phys.* **2015**, *142*, 244103.
- (72) Labat, F.; Le Bahers, T.; Ciofini, I.; Adamo, C. First-principles modeling of dye-sensitized solar cells: challenges and perspectives. *Acc. Chem. Res.* **2012**, *45*, 1268–1277.